Appl Magn Reson (2016) 47:321–334
DOI 10.1007/s00723-015-0748-2

Applied
Magnetic Resonance

NMR Applications for Polymer Composite Materials Moisture Uptake Investigation

V. M. Bouznik[1,2] · E. V. Morozov[3,4] · I. A. Avilova[1,5] · V. I. Volkov[1,5]

Received: 30 September 2015 / Revised: 23 November 2015 / Published online: 6 January 2016

Abstract The ^{1}H nuclear magnetic resonance (NMR) spectroscopy, NMR imaging, and pulsed field gradient NMR (PFG NMR) were applied for comparative study of moisture–polymer composite materials (PCM) interaction. The water uptake in PCM reinforced by aramid and carbon fibers was measured by NMR spectroscopy techniques. The aramid fiber-reinforced PCM absorbs water more intensively compared with PCM reinforced by carbon fiber, but both of them are retaining water inside of pores without formation of chemical bonds. Using NMR imaging the spatial distribution of water absorbed was visualized; preferable water pathways and influence of surface treatment on water-resistant properties were revealed. It was found that the surface rough treatment sufficiently improves the water absorption, but penetration of water molecules is still occurring only through the surfaces and it happens within a thin layer. PFG NMR technique revealed influence of pore structure on moisture–PCM interaction; it was found that additionally to strong hydrophobic properties of carbon fiber, the smaller total volume of pores sufficiently decrease the water uptake. Results achieved in this work demonstrate efficiency of NMR methods applied all together for investigation of PCM, and information obtained is practically important when designing advanced PCM with required properties.

✉ E. V. Morozov
morozov_if@mail.ru

[1] Institute of Problems of Chemical Physics RAS, Chernogolovka, Russia

[2] All-Russian Scientific Research Institute of Aviation Materials, Moscow, Russia

[3] Kirensky Institute of Physics SB RAS, Krasnoyarsk, Russia

[4] Institute of Chemistry and Chemical Technology SB RAS, Krasnoyarsk, Russia

[5] Science Center in Chernogolovka of the Russian Academy of Sciences, Chernogolovka, Russia

1 Introduction

Polymer composite materials (PCM) are being increasingly employed for advanced structural applications in many industries [1, 2]. The most widely spread PCM are consisted of epoxy-based matrices and reinforcing fiber [2]. These composites are used due to their favorable properties, including high strength-to-weight ratio, good corrosion and fatigue resistance, and relative ease of processing into complex integrated structures. It is recognized, however, that the mechanical properties of PCM are influenced by the presence of moisture: water molecules, as well as low-molecular substances, are able to move in a polymeric binder and change its physical properties, even in small quantities of the order of 5 wt% or less [3–6]. Moisture absorption in polymer composite parts can cause weight gain, hygroscopic dimensional changes, and material degradation. Accordingly, it is important to study moisture absorption behavior in order to estimate not only the consequences that the moisture absorbed may have, but also how this moisture uptake can be minimized.

Moisture absorption in polymer composite materials has been extensively investigated experimentally in the last few decades. Therefore, the mechanisms of absorption, effects of chemical structure of polymer as well as moisture level of environment on stability of materials now are generally revealed [7–13]. To achieve that, a number of methods were successfully employed: mechanical testing, thermal and gravimetric analyses, Fourier transform infrared (FTIR) spectroscopy, optical and scanning electron microscopy (SEM), etc. [14–18]. Nevertheless, there is still a little knowledge about some problems such as influence of moisture on the degradation of fiber–matrix interface, role of the surface treatment in water uptake, behavior of the water molecules inside the porous network, etc. It is evident that a new approach is required here to provide the better understanding of PCM–moisture interaction. And this approach should involve the different scales of characterization, bringing information on molecular level into correlation with that observed for bulk samples of composites.

In this article, three complementary nuclear magnetic resonance (NMR) techniques are proposed to employ for tracking the absorption of moisture by PCM over an extended period of time. For this aim, the ^{1}H NMR spectroscopy, NMR imaging (MRI), and pulsed field gradient (PFG) NMR techniques were applied all together to study two different samples of PCM. It should be mentioned that each of NMR techniques used in this article was applied before for investigation of solid polymers. For example, NMR spectroscopy was proved efficient and informative technique for determination of chemical structure and dynamic properties of polymer network [19–22], while pulsed field gradient (PFG) NMR is a well-known tool for investigation of transport properties, determination of pores geometry, and tracking the behavior of free and bound water in porous network [23–33]. MRI method, though, has been utilized only in a few works [34–37] because of its technical limitations: as a rule, the solid polymer composites have extremely short relaxation time (broad spectral line) that in turn requires applying of the strong gradients coupled with necessity to use special pulse sequences [38, 39]. Nevertheless, this method offers many advantages: MRI is nondestructive, accurate,

and rapid enough technique that allows a measurement to be taken on a sample without significantly disturbing the absorption process. Consequently, combination of MRI with NMR spectroscopy and diffusion measurements yields a very efficient approach that was used in this work for the first time.

2 Experimental Section

2.1 Samples

The materials used in this study were polymer composites VKO-19 consisted of aramid fiber "Rusar"/epoxy-balanced woven fabric prepreg [40] (sample 1) and KMU-11TR consisted of carbon fiber/epoxy-balanced woven fabric prepreg (sample 2), both produced in ARSRIAM. The laminated plates formed under pressure of 0.7 MPa were cut with a diamond saw into individual specimens having the dimensions of 2 mm × 10 mm × 30 mm. All longitudinal side surfaces were formed slick and left without special coating. The one of the crosscut side surface was treated by rasp to make it rough, and the opposite side was simply formed by mechanical demolition that yielded cracks; both these surfaces were considered prone to preferable water absorption as compared to the longitudinal surfaces. For imaging experiments, the PCM strips were used as they are, while for spectroscopic and diffusion measurements they were shredded into small shavings (about 0.5 mm length).

2.2 Equipment and Methods

The ^{1}H high-resolution NMR spectra were recorded on Bruker Avance-III-500 MHz spectrometer. The self-diffusion coefficients were measured on ^{1}H nuclei by pulsed field gradient technique at the frequency 400.22 MHz. The measurements were carried out on Bruker Avance-III-400 NMR spectrometer, equipped with the diff60 gradient unit. The pulsed field gradient-stimulated echo sequence was used. The gradient strength was varied linearly in 64 steps within a range from 0.1 to 27 T/m value. The integrated intensities of spectrum lines were used to obtain the dependence of echo signal attenuation $A(g)$ on the square of pulsed magnetic field gradient amplitude g^2 (diffusion decay). The gradient pulse duration (δ) was 1 ms, the interval between gradient pulses (Δ) varied in range of 20–1000 ms.

The imaging experiments were carried out using an NMR imaging installation based on a Bruker Avance DPX 200 console and superconducting magnet with an 89-mm diameter vertical bore, water-cooled, and self-shielded Bruker gradient set (with maximum gradient strength up to 292 mT/m); probe PH MINI 0.75, 38-mm internal diameter birdcage coil tuned and matched to ^{1}H nuclear resonance frequency of 200.13 MHz; and a console operated with Paravision 4.0 software. Slice non-selective 2D NMR images were acquired using single point imaging (SPI) technique. It should be mentioned here that the echo-based imaging techniques would be more informative when applied to study the PCM samples, but they require quite long echo time parameter (>1.5 and >3.4 ms for gradient and spin

echo techniques, respectively). These values are longer than T_2 time of the samples (<1 ms), which makes echo-based techniques application inappropriate: acquisition time becomes enormous and images will represent only the most mobile water molecules on the surface. The parameters of image acquisition were as follows: field of view (FOV) of 40 mm, matrix of 64 × 64 pixels, repetition time of 5 ms, dephasing time of 0.1 ms, acquisition time of few hours (depending on sample).

In addition to actual proton spectra obtained in 5 mm NMR ampoule for shredded samples, the whole-sample spectra were acquired using facilities of MRI scanner. Due to short relaxation time of the PCM samples, the spectra recorded using "liquid-state" conditions (the power of amplifiers supplied by MRI scanner is not enough for generating of the short and strong radiofrequency pulses needed for excitation of broad lines) cannot be employed for quantitative measurements. Nevertheless, these distorted spectra still keep all necessary structural information and can be used for qualitative estimation. Therefore, it allows achieving important information about water uptake for bulk samples before their study in shredded form.

PCM interaction with moisture was provided by two different ways: (1) sample strips and shavings were exposed to humid environment for extended period of time, and (2) they were immersed into distilled water for different periods of time. For spectroscopic and diffusion measurements, the samples were in contact with water vapor of saturated salt water solutions of NaBr (58 % relative humidity) and NaCl (75 % relative humidity). For imaging experiments, the samples were in contact with water vapor within the humidity chamber. Temperature during PCM–moisture interaction was maintained about 25 °C except the shavings of KMU-11TR sample, which were soaked in water at 80 °C for diffusion measurements. Experiments were carried on until samples having reached the constant weight and were conducted for various moisture content.

3 Results and Discussion

3.1 ^{1}H Spectroscopy Results

The whole-sample spectrum of sample 1 strip demonstrates presence of broad line that is typical for solid polymers [19] (Fig. 1, red line). This line contains the signal of protons from both the polymer network and residual water absorbed during sample preparation. Two-day long interaction of sample 1 with humid atmosphere results in substantial increasing of line intensity: water molecules actively penetrate into the sample (Fig. 1, green line). After that, the same sample immersed into the water for 4 days long demonstrates further increasing of amount of absorbed water (Fig. 1, blue line). Ratio of signal intensities presented in Fig. 1 is 1:2:3. Results of this experiment evidently show water penetration into the sample even despite of water-resistant properties addressed to these materials. High water absorption in sample 1 revealed by whole-sample spectra could have been a consequence of low quality of surfaces: they are not coated at all and two of them are additionally treated to improve absorbance.

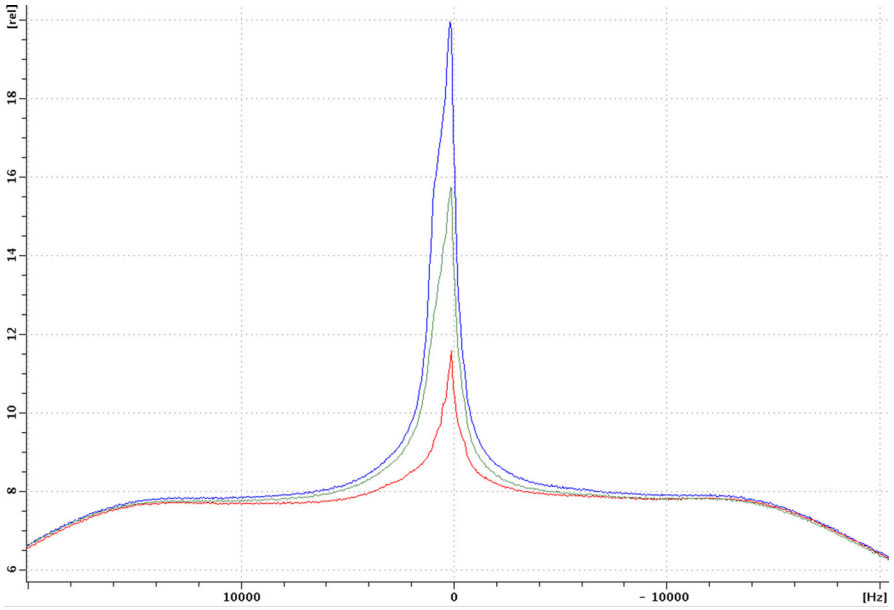

Fig. 1 Whole-sample ^{1}H spectra of sample 1 strip: initial spectrum (*red line*), after 2 days of interaction with humid atmosphere (*green line*), after 4 days of soaking in water (*blue line*) (color figure online)

As compared to the strip, the shredding of PCM sample leads to sufficient increasing of surface area and, consequently, should result in huge water absorption. Actual proton spectra of shavings exposed to humid atmosphere with various moisture contents are presented in Fig. 2. Generally, there is a good agreement with spectra obtained for the strips: the signal intensity increases as water penetrates into the shavings. One more effect, however, can be observed: increasing of water content results in not only growth of signal, but also the line itself becomes narrower. It means that the water molecules in pores of material become mobile as their amount increases. A very long exposure of shavings to humid atmosphere (with 100 % relative humidity) makes water to be condensed on the surface; narrow line in Fig. 2(5) vanishes after removing of water by blotting paper.

Results of experiments with sample 2 strips revealed a relatively weak interaction of PCM with water. Sufficient water absorption on the whole-sample spectra was found only after 6 days of exposure to humid atmosphere. But the spectrum of sample 2 left in open air even for the short time (few hours) demonstrates decreasing of the signal (Fig. 3). In this case a relatively weak bounding of water molecules cannot retain them inside the sample and water is evaporating freely. Long time immersing of sample 2 strip in distilled water surprisingly has no strong effect on signal intensity and its line is almost the same as that for sample exposed to humid atmosphere.

Actual proton spectra of sample 2 shavings exposed to humid atmosphere with different moisture content confirm that the signal intensity is weakly affected by either moisture content or time of exposure (Fig. 4, to compare with Fig. 2). This

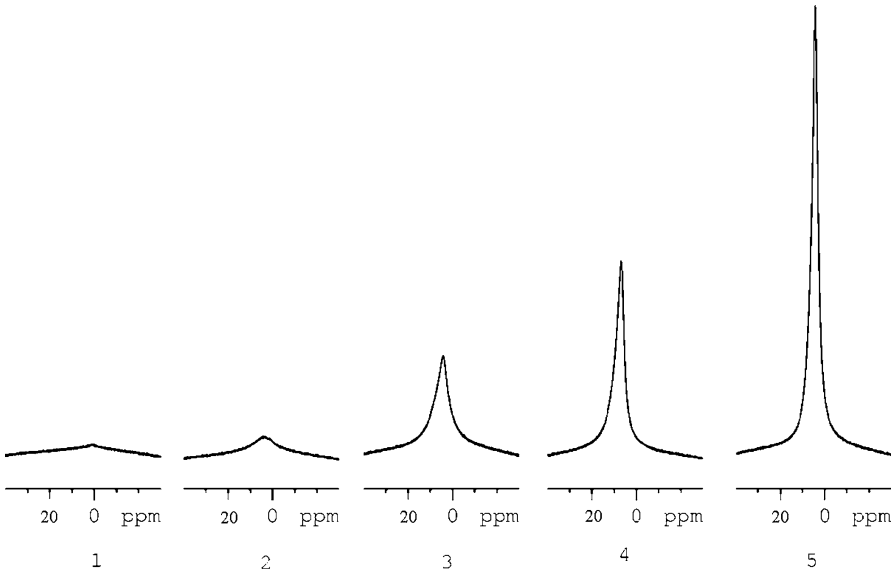

Fig. 2 ^{1}H spectra of sample 1 shavings exposed to humid atmosphere with various moisture contents: *1* initial spectrum (sample dried at 80 °C), *2* 58 % relative humidity (NaBr saturated salt water solution, for 11 days), *3* 75 % relative humidity (NaCl saturated salt water solution, for 11 days), *4* 100 % relative humidity (for 11 days), *5* 100 % relative humidity (for 39 days). The chemical shifts are measured relatively the bulk water signal

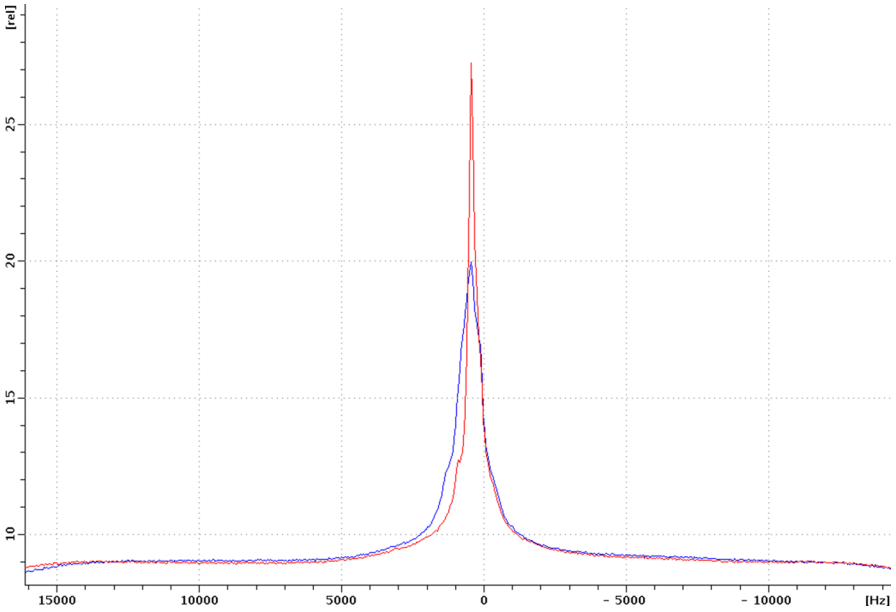

Fig. 3 Whole-sample ^{1}H spectra of sample 2 strip: spectrum after 6-day long interaction with humid atmosphere (*red line*), spectrum of the same strip after 2 h long left in open air (*blue line*) (color figure online)

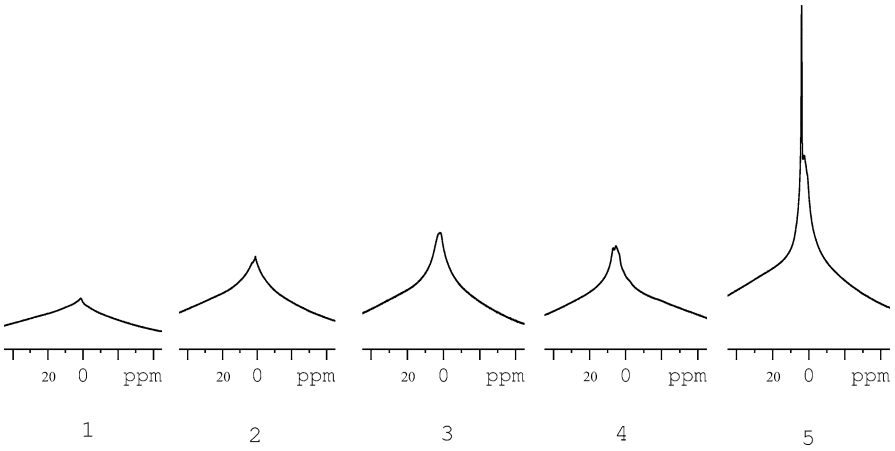

Fig. 4 ^{1}H spectra of sample 2 shavings exposed to humid atmosphere with different moisture content: *1* initial spectrum (sample dried at 80 °C), *2* 58 % relative humidity (NaBr saturated salt water solution, for 11 days), *3* 75 % (NaCl saturated salt water solution, for 11 days), *4* 100 % (for 11 days), *5* 100 % (for 39 days). The chemical shifts are measured relatively the bulk water signal

behavior can be accounted for the higher water-resistant (hydrophobic) properties of materials used for PCM preparation: pore space is able to absorb a very small amount of water without strong bounding, in result water molecules penetrate quite fast in both directions. It is worth noting that the chemical shift of the lines in spectra are not affected by amount of water absorbed and is almost the same as for water molecules in bulk. This fact also indicates that there are no chemical bonds between the water molecules and polymer network.

It is evidently demonstrated that ^{1}H spectroscopy is able to reveal water uptake and influence of PCM properties on extent of water absorption. But there is no information about preferable water localization inside the samples and its pathways. To address this problem, the NMR imaging was applied.

3.2 NMR Imaging Results

As it was established by ^{1}H spectroscopy, both dry samples of PCM demonstrate presence of protons, which are mobile enough to provide the image acquisition. Low signal intensity, though, makes this procedure very time-consuming due to a huge number of scans needed for reliable visualization. Images acquired cannot be analyzed carefully due to the strong noise presented there but rather homogeneous signal distribution over the strips was observed.

PCM–moisture interaction sufficiently increases amount of mobile water molecules inside the sample that is expected to increase the signal-to-noise ratio on the images. As result, the visualization becomes more reliable: images of sample 1 strip after interaction with moisture are presented in Fig. 5 (the signal intensity of images increases with water concentration inside the sample). It can be seen that signal intensity on the crosscut sides of the strip is more pronounced as compared to

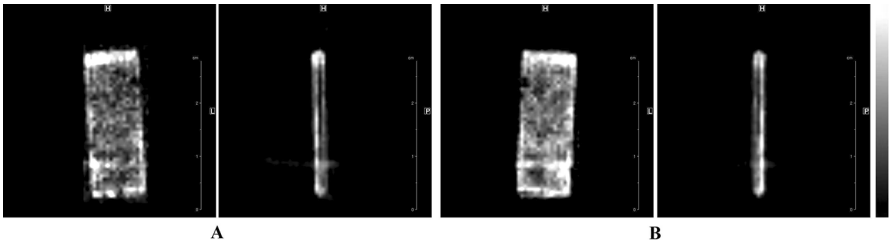

Fig. 5 NMR images of the sample 1 strip after interaction with moisture; **a** 48 h long of exposure to humid atmosphere, **b** 48 h long of soaking in water. Images are presented in two orthogonal directions

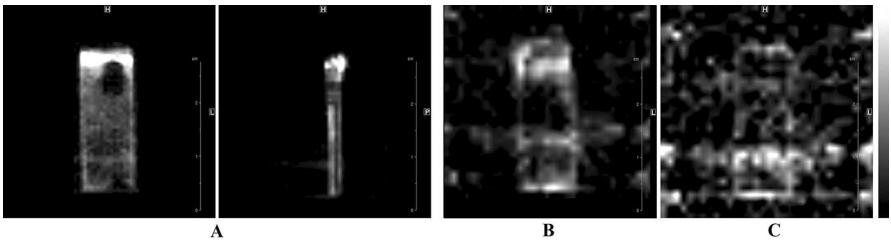

Fig. 6 NMR images of the sample 1 strip after 48 h long of soaking in water (**a**), images of the sample 2 strip after 6 days long of exposure to humid atmosphere (**b**) and 6 days long of soaking in water (**c**)

that on the longitudinal sides, according to the methods of surface treatment. Microcracks formed during the mechanical demolition and rasp treatment substantially increase the transport properties of the surfaces and act as promoters for active water penetration; slick surfaces proved to be water-resistant even being uncoated. Long time soaking of the strips leads to more intensive water absorption in comparison with that found for the strips exposed to humid atmosphere, but a thin layer with very low signal intensity still can be found inside the strip (it can be seen well on the transverse images, Fig. 5). Therefore, this layer is considered to be waterless due to its own water-resistant features as well as low transport properties of the slick surfaces.

It is well known that epoxy matrix in the PCM sample absorbs water more intensively than the reinforcing fiber [17, 41]. Owing to this fact, in some cases NMR imaging is able to visualize the structural defects of PCM strip: inhomogeneous distribution of epoxy binder within the strip may result in formation of waterless regions in wet samples (Fig. 6a, the layered structure of the strip can be clearly observed). This result is in agreement with assumption about the key role of epoxy matrix and epoxy-fiber surface in providing water transport inside the samples [37].

Influence of reinforcing fiber material on the water-resistant properties of PCM was demonstrated well in NMR imaging experiments with sample 2. Long time interaction of sample 2 strip with moisture revealed insufficient water absorption (Fig. 6b). Moreover, sample exposure to humid atmosphere appears more efficient

in terms of absorption than sample soaking in water during the same time. This effect is likely caused by high surface tension of the liquid water, that additionally to hydrophobic properties of the sample results in low wetting of the surface while the humid atmosphere is free from this restriction. Eventually crosscut sides only are found to be wet, where the surface was damaged noticeably. Advanced hydrophobic properties of carbon fiber sufficiently restrict water penetration along epoxy-fiber surface as compared to sample 1. In result, water molecules are not migrating deeply into the strip and they freely evaporate when sample becomes exposed to dry air again.

3.3 PFG NMR Results

Spectroscopic data allowed qualitative and quantitative estimation of the water uptake while MRI technique provided information about spatial distribution of water absorbed and its preferable pathways for penetration. The results, however, suffer from the lack of information about dynamic properties of the absorbed water. The PFG NMR technique was applied for measuring the water self-diffusion coefficients. For the molecules undergoing unhindered isotropic Brownian motion, the attenuation of spin echo signal (diffusion decay) $A(g)$ is described by the following equation [25–34]:

$$A(g) = \exp(-\gamma^2 \cdot g^2 \cdot \delta^2 \cdot t_d \cdot D_s), \tag{1}$$

where γ is gyromagnetic ratio, $t_d = \Delta - \delta/3$ is effective diffusion time, D_s is self-diffusion coefficient, g and δ are the amplitude and duration of magnetic field pulse, respectively, Δ is the interval between gradient pulses. For binary or multi-component system, which contains i types of water molecules with different diffusion coefficients, the resulting diffusion attenuation (Eq. 1) transforms into expression:

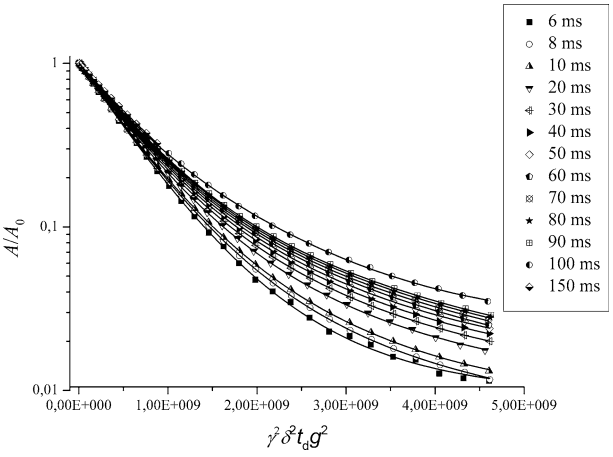

Fig. 7 Diffusion decays of sample 1 shavings soaked in water during 14 days long for different values of diffusion time; t_d which is indicated in figure insertion

$$A(g) = \sum_{i=1}^{m} p_i \cdot \exp(-\gamma^2 \cdot g^2 \cdot \delta^2 \cdot t_d \cdot D_{si}), \quad (2)$$

where D_{si} ($i = 1, 2, 3\ldots$) and p_i self-diffusion coefficients and their partial fractions, respectively. These parameters can be evaluated from diffusion attenuation directly in case of slow exchange between the water molecules presented in different states (with different motilities). Additionally, in case of restricted water diffusion, the pore size may be estimated from the dependence of D_s vs. t_d. The detail of pore size calculations are given in [29–33].

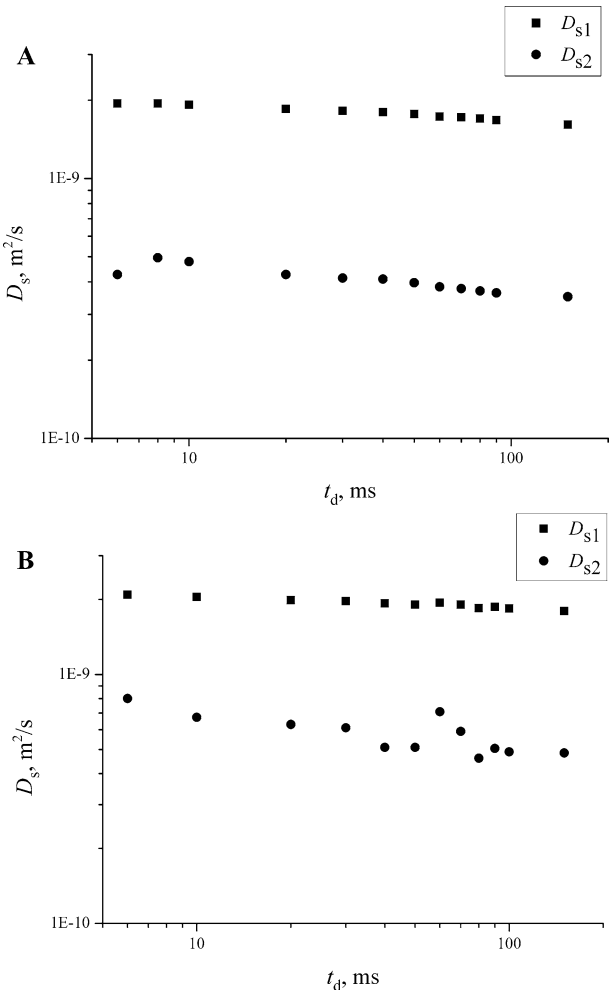

Fig. 8 Dependences of self-diffusion coefficients D_{s1} and D_{s2} vs. diffusion time t_d for PCM samples 1 (**a**) and 2 (**b**). The *error bars* are 10 %

As it was described above, the PCM sample 1 absorbs water well mainly due to its epoxy-based matrix. Diffusion decay curves of sample 1 shavings soaked in water during 14 days are presented in Fig. 7. These dependences are biexponential, indicating the presence at least of two types of water characterized by self-diffusion coefficients D_{s1} and D_{s2}. Self-diffusion coefficient D_{s1} weakly depends on diffusion time and its value is about 2.0×10^{-9} m^2/s (Fig. 8a). This value is close to the bulk water self-diffusion coefficient (2.3×10^{-9} m^2/s); so this type of water should be referred to bulk (free) water, freely diffusing between the shavings and their smaller compartments. Self-diffusion coefficient D_{s2} depends on diffusion time and its value 4.0×10^{-10} m^2/s at $t_d = 8$ ms is sufficiently lower than D_{s1} (Fig. 8a). Einstein relation $D_{s2} = \alpha^2/6t_d$ allows to estimate the scale of confinement of translational motion: random walk distance α which water molecules diffuse before reaching the walls of the pore is about 4.4×10^{-6} m. Therefore, this type, in turns, should be referred to bound water closed within the porous network. Partial fractions ratio of free and bound water is very high, which is expected due to relatively low amount of water absorbed by PCM sample. Long time soaking of sample shavings in hot water yields the same type of diffusion behavior, so there is no significant influence as compared to results of room temperature experiments.

The diffusion decays of sample 1 shavings exposed to humid atmosphere (with relative humidity of 100 %) during 10 days long are presented in Fig. 9. All of them obviously contain more than one component and can be fitted well by sum of three exponents. It is worth noticing that this fitting is rather simplified, the most likely there is a distribution of diffusion coefficients according to physical pores size distribution. Though, evaluating three distinct types of diffusion coefficients makes it easier to characterize the PCM samples. Diffusion coefficients and their partial fractions evaluated from experimental attenuation curves are listed in Table 1.

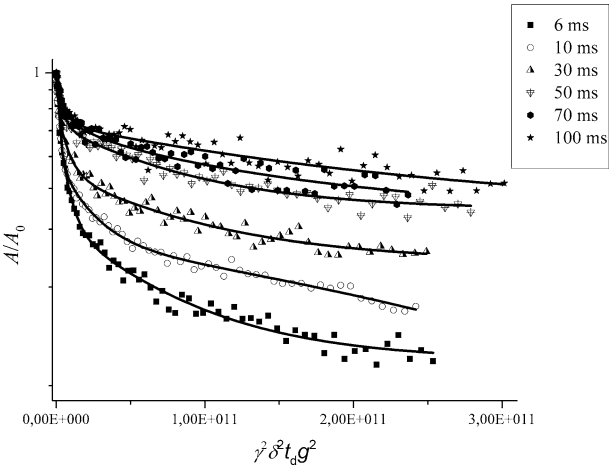

Fig. 9 Diffusion decays of sample 1 shavings exposed to humid atmosphere during 10 days long for different values of effective diffusion time; t_d is indicated in figure insertion

In contrary to those samples which were soaked in water, samples' exposure to humid atmosphere results in NMR signal coming from water molecules only absorbed by material. In case of liquid water having directly contacted with the sample surface, there is a relatively fast exchange between the water molecules in pores and bulk. Therefore, the apparent diffusion coefficient becomes averaged over all contributions from pores size distribution presented in the system [26].

The value of average self-diffusion coefficient D_s is given by Eq. 3:

$$\bar{D}_s = \sum_{i=1}^{m} D_{si} \cdot p_i. \tag{3}$$

In result, presence of only two diffusion coefficients (corresponding to water molecules in pores and bulk) generates the biexponential attenuation curves. When sample surface is contacting with humid atmosphere, the exchange of water

Table 1 Self-diffusion coefficients (D_{s1}, D_{s2}, D_{s3}) and their partial fractions (p_1, p_2, p_3) of sample 1 shavings exposed to humid atmosphere (with relative humidity of 100 %) for different values of effective diffusion time t_d

t_d (ms)	D_{s1} (10^{-10} m^2/s)	p_1	D_{s2} (10^{-11} m^2/s)	p_2	D_{s3} (10^{-13} m^2/s)	p_3
6	3.4 ± 0.3	0.56 ± 0.05	2.5 ± 0.3	0.28 ± 0.05	5.0 ± 0.5	0.16 ± 0.05
10	4.0 ± 0.4	0.50 ± 0.05	2.6 ± 0.3	0.24 ± 0.05	8.5 ± 0.6	0.26 ± 0.05
20	4.3 ± 0.4	0.50 ± 0.05	2.6 ± 0.3	0.28 ± 0.05	7.5 ± 0.6	0.22 ± 0.05
30	3.2 ± 0.3	0.44 ± 0.05	2.0 ± 0.3	0.24 ± 0.05	5.3 ± 0.5	0.32
50	3.3 ± 0.3	0.30 ± 0.04	2.0 ± 0.3	0.23 ± 0.05	8.7 ± 0.7	0.47
70	2.4 ± 0.3	0.28 ± 0.04	1.5 ± 0.2	0.20 ± 0.05	8.0 ± 0.7	0.52
100	2.1 ± 0.2	0.30 ± 0.04	1.5 ± 0.2	0.70 ± 0.05		

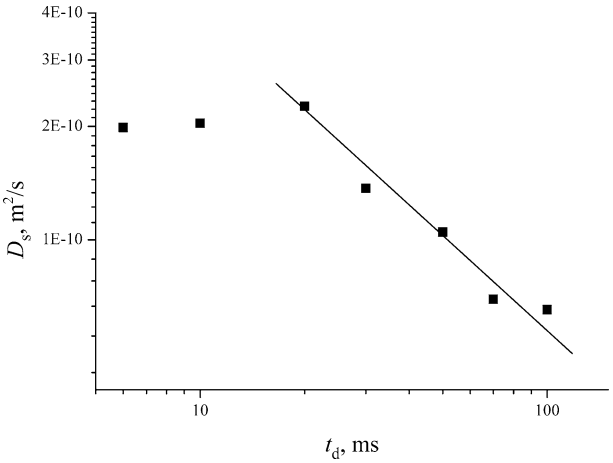

Fig. 10 Dependence of averaged self-diffusion coefficient vs. diffusion time for sample 1 shavings exposed to humid atmosphere during 10 days long. The *error bars* are 10 %

molecules between pores and environment is relatively slow; so the delay of water molecules inside the pores results in multi-component attenuation curves.

Averaged self-diffusion coefficient of sample 1 shavings exposed to humid atmosphere is found depends on diffusion time in the same manner as it was observed for that sample 1 soaked in water (Fig. 10): analysis gives the same value of random walk distance of 4.5×10^{-6} m.

Diffusion attenuation curves of sample 2 shavings were obtained only after long time soaking of this sample in hot water (80 °C). Analysis of the curves revealed the biexponential behavior, which is similar to those found in sample 1. Self-diffusion coefficients D_{s1} and D_{s2} correspond to free and bound water, relatively, and their values are presented in Fig. 8b for different diffusion times. Estimated random walk distance is slightly longer (6.7×10^{-6} m at $D_{s2} = 7 \times 10^{-10}$ m^2/s, $t_d = 10$ ms) than that found for sample 1. It is worth noting that pores in sample 2 appear bigger than those in sample 1 but their total volume is smaller. This suggestion is consistent well with the results achieved by two other techniques: water molecules easily diffuse within the sample 2 but amount of water absorbed is very small.

4 Conclusions

This work introduces a new approach for investigation of moisture–polymer composite materials interaction. This approach involves three complementary NMR techniques working all together: NMR spectroscopy (including whole-sample application), NMR imaging, and pulsed field gradient NMR. Therefore, NMR spectroscopy allowed revealing of water uptake as well as studying of absorbed water properties, behavior, and absorption kinetic. The aramid fiber-reinforced PCM was found to absorb water more intensively as compared to PCM sample reinforced by carbon fiber, but both of them are retaining water inside pores without formation of chemical bonds. NMR imaging applied sufficiently improved understanding, giving the information about spatial distribution of water absorbed inside the sample, its preferable pathways, and influence of surface treatment and/or sample composition on water-resistant properties. In particular, rough treatment of the surfaces was found to improve sufficient absorption of water, but penetration of water molecules is still occurring only through the surfaces and it happens within a thin layer which is the most likely formed by epoxy-based binder. Influence of pore structure on moisture–PCM interaction was revealed using PFG NMR technique which provided information about dynamic properties of water inside the pores. Therefore, it was found that in addition to strong hydrophobic properties of carbon fiber itself, the smaller total volume of pores sufficiently decrease the water uptake. Results achieved in this work evidently proved NMR methods to be very efficient when applied all together for investigation of PCM aging and/or degradation in humid environment. This approach also can be used for practical applications when developing advanced PCM with the required properties.

Acknowledgments This research was performed with the financial support of Russian Foundation for Basic Research (project no. 14-29-10178 ofi_m).

References

1. A. Kelly, *Concise encyclopedia of composite materials* (Pergamon Press, Oxford, 1989)
2. M. Zoghi, *The International Handbook of FRP Composites in Civil Engineering* (CRC Press, New York, 2013)
3. Y.C. Lin, X. Chen, Polymer **46**, 11994 (2005)
4. F. Ellyin, R. Maser, Compos. Sci. Technol. **64**, 863 (2004)
5. M. Akay, S. Kong Ah Mun, A. Stanley, Compos. Sci. Technol. **57**, 565 (1997)
6. M. Cotinaud, P. Bonniau, A.R. Bunsell, J. Mater. Sci. **17**, 867 (1982)
7. Y.C. Lin, X. Chen, Chem. Phys. Lett. **412**, 322 (2005)
8. A. Naceri, Strength Mater. **41**(4), 444 (2009)
9. B.C. Ray, J. Colloid Interface Sci. **298**, 111 (2006)
10. B. Abdel-Magid, S. Ziaee, K. Gass, M. Schneider, Compos. Struct. **71**, 320 (2005)
11. H.B. Hopfenberg, J. Membr. Sci. **3**, 215 (1978)
12. M. Al-Harthi, K. Loughlin, R. Kahraman, Adsorption **13**, 115 (2007)
13. D.A. Bond, J. Compos. Mater. **39**(23), 2113 (2005)
14. S. Popineaua, M.E.R. Shanahan, Int. J. Adhes. Adhes. **26**, 363 (2006)
15. I. Cerny, R.M. Mayer, Compos. Struct. **92**, 2035 (2010)
16. S. Cotugno, G. Mensitieri, Macromolecules **38**, 801 (2005)
17. E. Kalfon, H. Harel, G. Marom, E. Drukker, A.K. Green, I. Kressel, Polym. Compos. **26**(6), 770 (2005)
18. I. Hamerton, J.N. Hay, B.J. Howlin, J.R. Jones, S-Yu. Lu, G.A. Webb, M.G. Bader, Polym. Bull. **38**, 433 (1997)
19. J.L. Koenig, *Spectroscopy of Polymers* (American Chemical Society, Washington, 1992)
20. T.L. Weeding, W.S. Veeman, L.W. Jenneskens, H. Angad Gaur, H.E.C. Schuurs, W.G.B. Huysmans, Macromolecules **22**(2), 706 (1989)
21. J.E. Gambogit, F.D. Blum, Macromolecules **25**, 4526 (1992)
22. M.A. Smirnov, V.P. Tarasov, V.M. Buznik, A.S. Kantaev, A.N. D'yachenko, J. Struct. Chem. **54**(1), 174 (2013)
23. W.S. Price, *NMR Studies of Translational Motion. Principles and Applications* (University Press, Cambridge, 2009)
24. P.T. Callaghan, *Translational Dynamics and Magnetic Resonance. Principles of Pulsed Gradient Spin Echo NMR* (University Press, Oxford, 2011)
25. V.I. Volkov, A.A. Marinin, Russ. Chem. Rev. **82**(3), 248 (2013)
26. A.I. Maklakov, V.D. Skirda, N.F. Fatkullin, *Self-Diffusion in Polymer Solutions and Melts* (Kazan State University Press, Kazan, 1987), p. 223. **(in Russian)**
27. I. Furo, S.V. Dvinskikh, Magn. Reson. Chem. **40**, 3 (2002)
28. V.I. Volkov, S.A. Korotchkova, H. Ohya, Q. Guo, J. Membr. Sci. **100**, 273 (1995)
29. C.-H. Cho, Y.-S. Hong, K. Kang, V.I. Volkov, V. Skirda, C.-Y.J. Lee, C.-H. Lee, Magn. Reson. Imaging **21**, 1009 (2003)
30. K.-J. Suh, Y.-S. Hong, V.D. Skirda, V.I. Volkov, C.-Y. Lee, C.-H. Lee, Biophys. Chem. **104**, 121 (2003)
31. I.A. Avilova, S.G. Vasil'ev, L.V. Rimareva, E.M. Serba, L.D. Volkova, V.I. Volkov, Russ. J. Phys. Chem. A **89**, 710 (2015)
32. P.P. Mitra, P.N. Sen, L.M. Schwartz, P.L. Doussal, Phys. Rev. Lett. **68**, 3555 (1992)
33. R.R. Valiullin, V.D. Skirda, S. Stapf, R. Kimmich, Phys. Rev. E. **55**, 2664 (1996)
34. P. Jezzard, C.J. Wiggins, T.A. Carpnter, L.D. Hall, P. Jackson, N.J. Clayden, N.J. Walton, Adv. Mater. **4**(2), 82 (1992)
35. J.H. Iwamiya, S.W. Sinton, Solid State Nucl. Magn. Reson. **6**, 333 (1996)
36. D.E. Axelson, A. Kantzas, A. Nauerth, Solid State Nucl. Magn. Reson. **6**, 309 (1996)
37. G. Kotsikos, A.G. Gibson, J. Mawella, Plastics Rubber Compos. **36**(9), 413 (2007)
38. G. LaPlante, A.V. Ouriadov, P. Lee-Sullivan, B.J. Balcom, J. Appl. Polym. Sci. **109**, 1350 (2008)
39. Zh Fang, D. Hoepfel, K. Winter, Magn. Reson. Imaging **19**, 501 (2001)
40. G.F. Zhelezina, I.V. Zelenina, N.A. Solov'eva, A.E. Raskutin, A.M. Gurevitch, *A Method for Producing of Structural Composite Material*, Russian Patent No. 2405675 (2009)
41. T.I. Glaskova, R.M. Guedes, J.J. Morais, A.N. Aniskevich, Mech. Compos. Mater. **43**(4), 377 (2007)